

# Hemodynamic and EEG Time-Courses During Unilateral Hand Movement in Patients with Cortical Myoclonus. An EEG-fMRI and EEG-TD-fNIRS Study

E. Visani · L. Canafoglia · I. Gilioli · D. Rossi Sebastiano · V. E. Contarino · D. Duran · F. Panzica · R. Cubeddu · D. Contini · L. Zucchelli · L. Spinelli · M. Caffini · E. Molteni · A. M. Bianchi · S. Cerutti · S. Franceschetti · A. Torricelli

Received: 24 March 2014 / Accepted: 17 September 2014 / Published online: 25 September 2014  
© Springer Science+Business Media New York 2014

**Abstract** Multimodal human brain mapping has been proposed as an integrated approach capable of improving the recognition of the cortical correlates of specific neurological functions. We used simultaneous EEG-fMRI (functional magnetic resonance imaging) and EEG-TD-fNIRS (time domain functional near-infrared spectroscopy) recordings to compare different hemodynamic methods with changes in EEG in ten patients with progressive myoclonic epilepsy and 12 healthy controls. We evaluated O<sub>2</sub>Hb, HHb and Blood oxygen level-dependent (BOLD) changes and event-related desynchronization/synchronization (ERD/ERS) in the  $\alpha$  and  $\beta$  bands of all of the subjects while they performed a simple motor task. The general linear model was used to obtain comparable fMRI and TD-fNIRS activation maps. We also analyzed cortical

thickness in order to evaluate any structural changes. In the patients, the TD-NIRS and fMRI data significantly correlated and showed a significant lessening of the increase in O<sub>2</sub>Hb and the decrease in BOLD. The post-movement  $\beta$  rebound was minimal or absent in patients. Cortical thickness was moderately reduced in the motor area of the patients and correlated with the reduction in the hemodynamic signals. The fMRI and TD-NIRS results were consistent, significantly correlated and showed smaller hemodynamic changes in the patients. This finding may be partially attributable to mild cortical thickening. However, cortical hyperexcitability, which is known to generate myoclonic jerks and probably accounts for the lack of EEG  $\beta$ -ERS, did not reflect any increased energy requirement. We hypothesize that this is due to a loss of inhibitory neuronal components that typically fire at high frequencies.

E. Visani (✉) · L. Canafoglia · I. Gilioli · D. R. Sebastiano · D. Duran · F. Panzica · S. Franceschetti  
Dipartimento di Neurofisiologia ed Epilettologia Diagnostica,  
Fondazione IRCCS Istituto Neurologico “Carlo Besta”, via  
Celoria 11, 20133 Milan, Italy  
e-mail: visani.e@istituto-besta.it

V. E. Contarino  
Dipartimento di Neuroradiologia, Fondazione IRCCS Istituto  
Neurologico “Carlo Besta”, Milan, Italy

R. Cubeddu · D. Contini · L. Zucchelli · A. Torricelli  
Dipartimento di Fisica, Politecnico di Milano, Piazza Leonardo  
da Vinci 32, 20133 Milan, Italy

L. Spinelli  
Istituto di Fotonica e Nanotecnologie, CNR, Piazza Leonardo da  
Vinci 32, 20133 Milan, Italy

M. Caffini · E. Molteni · A. M. Bianchi · S. Cerutti  
Dipartimento di Elettronica, Informazione e Bioingegneria,  
Politecnico di Milano, Via Golgi 39, 20133 Milan, Italy

**Keywords** Multimodal mapping · Time domain fNIRS · EEG-fMRI · Myoclonus

## Abbreviations

AUC	Area under the curve
BOLD	Blood oxygen level-dependent
CT	Cortical thickness
EEG	Electroencephalography
EMG	Electromyography
EPM1	Progressive myoclonic epilepsy 1A
ERD/ERS	Event-related desynchronization/ synchronization
fMRI	Functional magnetic resonance imaging
fNIRS	Functional near-infrared spectroscopy
FWE	Family wise error
FWHM	Full width at half maximum
GLM	General linear model
HHb	Deoxyhemoglobin

HRF	Hemodynamic response function
MDL	Minimum description length
MNI	Montreal Neurological Institute
MRI	Magnetic resonance imaging
NIR	Near-infrared
O <sub>2</sub> Hb	Oxyhemoglobin
ROI	Region of interest
SPM	Statistical parametric mapping
TD-fNIRS	Time domain functional near-infrared spectroscopy

## Introduction

Functional magnetic resonance imaging (fMRI) and functional near-infrared spectroscopy (fNIRS) are both used to measure hemodynamic responses coupled with neural activity, whereas electroencephalography (EEG) directly measures the electrical activity generated by the cerebral cortex.

Electroencephalography has a very high temporal resolution (in the order of milliseconds), but it is limited by spatial blur distortion and has a low spatial resolution. Despite its limited temporal resolution (1–2 s), fMRI has the advantage of greater spatial resolution and allows the whole brain mapping of function, but it only measures neuronal activity indirectly by assessing changes in deoxyhemoglobin paramagnetic properties, and the precise relationship between oxygen consumption and brain activity (i.e. neurovascular coupling) is still unclear (Logothetis et al. 2001). Functional fNIRS has a higher temporal resolution than fMRI (low spatial resolution) and is capable of directly measuring the concentration of both oxyhemoglobin and deoxyhemoglobin; it is also less affected by movement artefacts. Furthermore, it allows a more comfortable environment, which can be favorable in the case of subjects with neurological disorders. Although it is unsuitable for investigating hemodynamic changes in deep brain structures, it is very useful for functional studies of events primarily involving brain neocortex. All of these differences make fMRI and fNIRS complementary techniques that can be associated with EEG recordings to study physiological and pathological cortical neural activities.

We used matching hemodynamic (fMRI and fNIRS) and EEG recordings in patients with progressive myoclonic epilepsy type 1A (EPM1, MIM #254800), an hereditary autosomal recessive disorder that begins in late childhood and leads to worsening cortical myoclonus associated with mild ataxia, minimal or absent cognitive impairment, and rare generalized seizures (Shahwan et al. 2005). EPM1 patients show rare EEG epileptic paroxysms sometimes

associated with spontaneous myoclonus, while the EEG correlate of action-activated myoclonus is poorly recognizable by visual inspection but well detectable by spectral analysis and highly coherent with myoclonic EMG burst (Panzica et al. 2003; Panzica et al. 2014). Moreover, with respect to healthy subjects, EPM1 patients show characteristic changes in movement associated EEG event-related desynchronization/synchronization (ERD/ERS) in  $\alpha$  and  $\beta$  band, with the prominent finding of absent or extremely reduced beta-rebound at the movement end (Visani et al. 2006).

In a previous study (Visani et al. 2011), aimed at comparing EEG with hemodynamic changes, we applied event-related and block-design movement protocols during EEG-fMRI. Comparing EPM1 patients with controls we could regularly find consistent changes in the ERD/ERS pattern, but we were unable to detect difference in fMRI signals. In an attempt to clarify the reason for this dissociation, we simultaneously used multiple hemodynamic techniques and EEG recordings to investigate the correspondence between the time domain fNIRS (TD-fNIRS) and fMRI hemodynamic findings in EPM1 patients and controls, and the relationship between the hemodynamic time courses and ERD/ERS) behavior. TD-fNIRS was chosen because it is more sensitive and informative than classic fNIRS as it allows better separation of the contributions of surface and brain tissues, and a better assessment of physiological parameters (blood volume and oxygenation) (Torricelli et al. 2014). In order to improve the comparison of the different results, we concentrated on the cortical area showing the greater task related changes: i.e. a “functional” region of interest (ROI) rather than a pre-assigned anatomical ROI.

## Materials and Methods

### Subjects

The study involved ten right-handed EPM1 patients (three females; age  $36 \pm 10.2$  years, disease duration  $22.2 \pm 9.7$  years) and 12 right-handed healthy controls (four females; age  $32.2 \pm 10$  years). The diagnosis of EPM1 was hypothesised on the basis of its typical electro-clinical presentation and confirmed by the finding of a dodecamer expansion of the *cstb* gene (Virtaneva et al. 1997). The enrolled patients presented with mildly to moderately severe myoclonus (a score of two or three on a simplified rating scale, Magaudda et al. 2004) and were receiving similar anti-epileptic treatment: valproate (10), levetiracetam (3), topiramate (2), benzodiazepine (1), bromazepam (1), clonazepam (1), lamotrigine (1), phenobarbital (1), and piracetam (1).

The study was reviewed and approved by our local Ethics Committee and was conducted in compliance with the Declaration of Helsinki; all of the subjects gave their written informed consent to participate.

### Experimental Paradigm

The motor task consisted of a right hand grip (i.e. squeezing a soft ball) at a rate of 2 Hz guided by a metronome. After an initial 60 s resting period, 10 trials were carried out by alternating 20 s task and 20 s rest, followed by a recovery period of 30 s (Fig. 1a). Instructions about the movement and rest were given by presenting a picture on a screen, which always had a fixation cross in the centre. The total duration of the protocol was about 8 mins. The EEG-fMRI and EEG-TD-fNIRS data were acquired within a few hours on the same day.

### Data Acquisition

#### *EEG and TD-fNIRS Acquisition*

Electroencephalography signals were recorded by means of 19 Ag/AgCl surface electrodes placed on the scalp in accordance with the 10/20 International System. Electromyographic (EMG) activity was simultaneously recorded from pairs of Ag/AgCl surface electrodes placed bilaterally 2–3 cm apart over the flexor muscle of the right index finger; the EMG signal from the antagonist muscles of the EPM1 patients was recorded at the same time. The EEG and EMG signals were acquired using a Micromed Brain Quick digital system (Micromed SpA, Mogliano Veneto, Italy) at a sampling frequency of 512 Hz (band-pass filters: 1–200 Hz). The TD-fNIRS data were acquired using a multi-channel dual wavelength class I medical device developed by the Physics Department of the Politecnico of Milan (Contini et al. 2009) in which the light sources consist of two pulsed diode lasers operating at 690 and 820 nm with an 80 MHz repetition rate. The light pulses at two wavelengths were time multiplexed in different injection fibers by means of two independent optical switches. The delivery system allows up to 16 injection points with a mean power output of less than 1 mW, and up to 16 detection bundles to collect the remitted photons in four parallel detection chains equipped with multi-anode photomultipliers, amplifiers and boards for time-correlated single photon counting in order to acquire the distribution of photon time-of-flights.

In our experiment, a total of 15 detection bundles and eight light sources were positioned over the sensorimotor areas centred on C3 and C4 (Fig. 1b), and an in-house support was used to guarantee the stability of the contact between optodes and the subject's scalp after the correct

optode positioning had been checked by means of preliminary transcranial magnetic stimulation (MagVenture MagOption, Medtronic, Skovlunde, Denmark) mapping of the cortical hands motor area associated with real-time frameless neuronavigation (Softaxic, EMS, Bologna, Italy). The sequential illumination of pairs of light sources in the left and right hemisphere every 0.25 s allowed the acquisition of 30 measurement points (channels) with an overall acquisition time of 1 s.

#### *EEG-fMRI Acquisition*

Conventional MRI and fMRI were carried out using a 1.5 T scanner (Siemens MAGNETOM Avanto, Erlangen, Germany). Sagittal T1-weighted volumetric images were acquired using a magnetization-prepared gradient-echo sequence (TR = 1640 ms, TE = 2.12 ms, TI = 552 ms, flip angle = 12°, FOV = 256 × 256 mm, matrix = 256 × 256, slice-thickness = 1 mm, 160 slices), and the functional images were acquired using an axial gradient-echo echo-planar sequence (TR = 2,000 ms, TE = 50 ms, 2 × 2 mm<sup>2</sup> in-plane voxel size, 5 mm slice thickness, no gap 21 slices). The EEG data were acquired using an MR-compatible device (SD MRI 32, Micromed SpA, Mogliano Veneto, Italy) and a cap equipped with 30 sponge electrodes positioned in accordance with the 10/20 international system (sampling frequency: 1,024 Hz; band-pass filters: 1–200 Hz). An electrocardiogram (ECG) was also recorded by means of two electrodes applied in accordance with the DI Einthoven derivation. EMG activity was recorded through a pair of Ag/AgCl electrodes positioned 2–3 cm apart on either side of the flexor muscle of the right index finger. Scanning and cardiac artifacts were removed using the software provided with the EEG system (System Plus Evolution v.1.4.50, Micromed SpA). Gradient-switching and radio frequency artifacts in the EEG and EMG signals were removed by means of average model subtraction followed by adaptive filtering; the ballistocardiogram was subsequently removed using a similar approach, with each QRS complex being identified (Allen et al. 1998, 2000; Gray et al. 2009).

### Data Analysis

#### *TD-fNIRS Data*

The temporal changes in oxygenated hemoglobin (O<sub>2</sub>Hb) and deoxygenated hemoglobin (HHb) in the cortical regions were estimated using the method described in Contini et al. 2007, which is based on the use of a late time-gate in order to enhance the contribution of signals from the deeper cortical regions and reject the contribution from the superficial layers (i.e. the scalp and skull). Using a

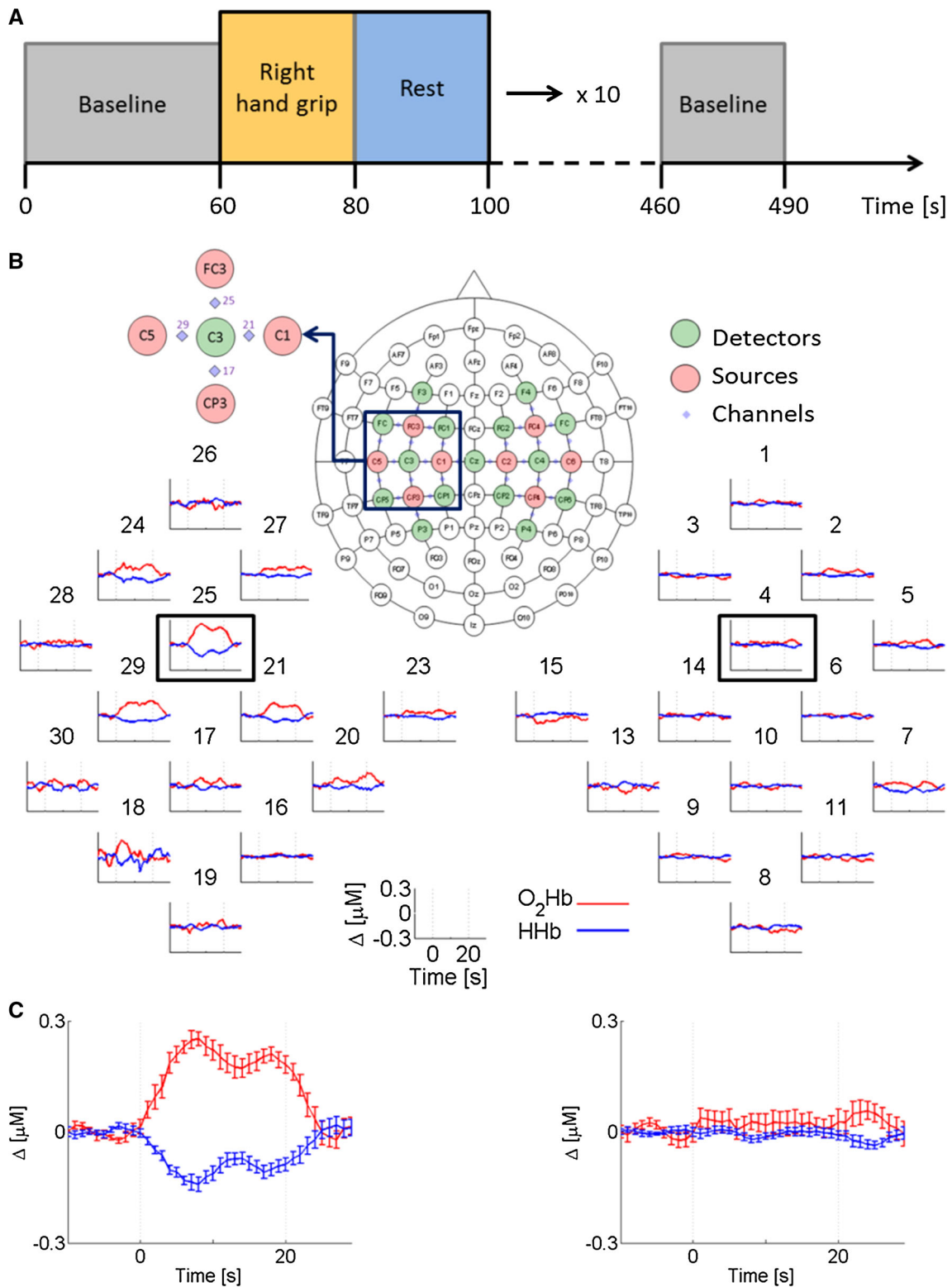


**Fig. 1** a Block-design motor protocol. b TD-fNIRS measurement with detail of the studied area (17, 21, 25 and 29 indicate the investigated channels). c O<sub>2</sub>Hb and HHb time courses in a representative healthy subject. The vertical bars represent the standard error

custom-written toolbox in MATLAB (R2012b, MathWorks Inc., Natick, MA, U.S.A.), the O<sub>2</sub>Hb and HHb signals were divided into epochs ranging from 10 s before to 30 s after the onset of each movement block, and then smoothed, de-trended and averaged over all of the trials. The most reactive channel (i.e. the channel showing the greatest difference between O<sub>2</sub>Hb and HHb values) was used for the analyses and comparisons. The value and latency of the maximal variation, and the area under the curve (AUC) during movement (0–20 s), were calculated for each hemoglobin species. In order to obtain individual and average activation maps comparable with those of the fMRI, the general linear model (GLM) was applied to the time courses of the changes in O<sub>2</sub>Hb and HHb concentration at individual and whole group level using NIRS-SPM software (Ye et al. 2009). Pre-processing algorithms were applied to the raw TD-fNIRS data using the internal routines of the software, with a detrending filter (Wavelet-MDL) being used to remove the global physiological dynamics (Jang et al. 2009). The GLM analyses were made using a series of consecutive boxcar functions co-involved with the hemodynamic response function (HRF) as regressor depending on the activity performed during the experiment. Statistical significance was expressed as t-contrasts for every channel with a threshold level of  $p < 0.05$  (uncorrected). Each channel's position was recorded over a reference MRI atlas in the Montreal Neurological Institute (MNI) coordinates system, and the points on the scalp were projected on the surface of a three-dimensional reconstruction of brain cortex. Statistical maps were obtained by interpolating the values of the t-statistics.

#### MRI Data

The cortex was reconstructed and parcellated using the Freesurfer image analysis suite, version 5.1 (<http://surfer.nmr.mgh.harvard.edu/>). The technical details of these procedures have been described in previous publications (Fischl et al. 2004; Han et al. 2006; Segonne et al. 2007). Parcel-wise analysis was made by averaging cortical thickness (CT) into each parcellated region (Desikan et al. 2006) and testing the differences within each parcellated region between the controls and patients using a *t* test with Bonferroni's correction for multiple comparisons. Vertex-wise analysis was made using a surface-based group analysis of Free Surfer's Qdec (version 1.4). The results were corrected for multiple comparisons by means of Monte Carlo simulation with a cluster wise probability of  $p < 0.05$ .

#### fMRI Data

In order to obtain activation maps, the fMRI data were pre-processed and analyzed using SPM8 software (Wellcome

Trust Centre for Neuroimaging, London, UK). Volumes were realigned using a rigid-body transformation, followed by slice-timing correction and normalization in the MNI space. Gaussian smoothing was performed using a 7 mm full-width at half-maximum isotropic kernel. The first-level individual analyses were made by means of GLM, entering the block function co-involved with the canonical SPM HRF as regressor (Friston et al. 1995). The effects were described on t-contrast maps using the family-wise error (FWE) correction for multiple comparisons with a voxel-level threshold of  $p = 0.05$ ; when this did not reveal any significant difference (no supra-threshold voxel using FWE correction), an uncorrected threshold of  $p < 0.001$  was considered. The ROI was the most significant activated cluster within the contralateral primary motor and somatosensory areas extracted from the activation maps. The time-course of the percentage change in the BOLD signal ( $\Delta$ BOLD) derived from the smoothed volume series was up-sampled to 10 Hz by means of spline interpolation, and averaged over all of the voxels within the ROI. The resulting signal was de-trended with a 10th degree polynomial, and subsequently divided into epochs ranging from 10 s before to 30 s after the onset of each movement. After subtracting the pre-movement average, the epochs were averaged. The value and time of the maximal variation, and the AUC of  $\Delta$ BOLD during movement, were determined.

#### EEG Data

Movement onsets were determined by manually tagging the beginning of the EMG burst at the start of each block of movements, and the EEG data were divided into epochs ranging from 10 s before to 30 s after the start of each movement. The ERD/ERS data were analysed using the EEG data and custom written software developed using the Matlab language (R2012b, Mathworks Inc., Natick MA, USA). Surface Laplacian estimate (Perrin et al. 1989) was applied to obtain reference-free and spatially sharpened EEG data. For each subject, the most reactive a- and b-band frequencies were determined in the 8–13 and 13–30 Hz ranges, by means of an iterative procedure. This allowed to maximize the alpha-ERD negative peak and the difference between the beta ERD negative peak and the ERS positive peak. Each epoch was digitally band-pass filtered in the  $-1$  to  $1$  Hz band centered on the most reactive a- and b-band frequencies by means of a zero-phase 512-point finite impulse-response filter. The filtered EEG signals were then squared, averaged over all epochs, and down-sampled with one data-point every 250 ms. The relative ERD/ERS values were expressed as percent power change, calculated with respect to mean power in the  $-4$  to  $-3$  s pre-movement reference period (Pfurtscheller and Lopes da Silva 1999). The statistical analyses were made on



**Table 1** Statistical test on hemodynamic measures

	EPM1 patients	Healthy subjects	<i>p</i>
<b>Hemodynamic data</b>			
AUC O <sub>2</sub> Hb <sub>act</sub> (μM·s)	0.993 ± 0.635	3.007 ± 1.243	0.002
AUC HHb <sub>act</sub> (μM·s)	0.939 ± 0.924	1.402 ± 0.637	n.s.
Max O <sub>2</sub> Hb <sub>act</sub> (μM)	0.117 ± 0.109	0.247 ± 0.087	0.014
Max HHb <sub>act</sub> (μM)	−0.096 ± 0.089	−0.130 ± 0.069	n.s.
AUC ΔBOLD (%·s)	741.57 ± 209.24	1275.5 ± 350.24	0.001
Max ΔBOLD (%)	5.17 ± 1.21	8.13 ± 2.37	0.004
<b>Cortical thickness</b>			
	EPM1 patients	Healthy subjects	<i>p</i>
<b>MRI data</b>			
Left paracentral (mm)	2.1 ± 0.1	2.4 ± 0.1	0.00005
Left precentral (mm)	2.2 ± 0.1	2.6 ± 0.1	<0.00001
Right paracentral (mm)	2.1 ± 0.1	2.4 ± 0.1	0.00002
Right precentral (mm)	2.2 ± 0.1	2.5 ± 0.1	<0.00001

AUC area-under-curve, Max value for maximal variation, n.s. not significant

the most reactive electrode (i.e. the electrode showing the highest ERD/ERS value) for both  $\alpha$ - and  $\beta$ -bands. For  $\alpha$  and  $\beta$  desynchronization, we calculated the AUC, the value, and the latency of the maximal deflection during the movement; for  $\beta$  synchronization, the same parameters were extracted in the 5 s after the movement stopped.

### Statistical Analysis

The measures extracted from each data category were compared between groups by means of the non-parametric Mann–Whitney U test, and correlations were analyzed using Spearman's rank correlation coefficient. All of the statistical analyses were carried out using Statistical Package for the Social Sciences software, version 14 (SPSS Inc., Chicago, IL, U.S.A). The data are reported as mean values ± SD.

For each data set, we applied thresholds correction implemented in the specific software used to analyze hemodynamic data (NIRS-SPM and SPM8) and imaging data (FreeSurfer).

## Results

### TD-fNIRS Data Analysis

One patient and two controls did not show any reliable activation, and were excluded from further analysis. TD-fNIRS detected significant functional activation in all of

the other subjects as an increase in O<sub>2</sub>Hb and a corresponding non-symmetrical decrease in HHb on the channels located on the hemisphere contralateral to the activated hand. Figure 1b shows the time courses of O<sub>2</sub>Hb and HHb in a representative control subject. In all subjects, the channel showing the greatest difference was located close to C3 (Fig. 1b). In all cases, after an initial increase in O<sub>2</sub>Hb and a delayed decrease in HHb, the activation curves reached a plateau that lasted throughout the active period of the task, and then returned to baseline about 8–9 s after the onset of the movement block (EPM1 patients O<sub>2</sub>Hb and HHb: 7.2 ± 3.4 s and 7.0 ± 3.6 s; controls 8.9 ± 2.8 s and 7.9 ± 3.3 s). The temporal offset of HHb in relation to O<sub>2</sub>Hb was 1–2 s and, in all subjects, the changes in HHb were smaller than those in O<sub>2</sub>Hb. In comparison with the controls, EPM1 patients showed less activation, corresponding to a smaller increase in O<sub>2</sub>Hb and decrease in HHb (Table 1 and Fig. 2). Both the maximal value and AUC of O<sub>2</sub>Hb were significantly lower in the EPM1 patients (0.12 ± 0.10 vs 0.25 ± 0.09, *p* = 0.014; and 0.99 ± 0.63 vs 3.0 ± 1.24, *p* = 0.002). The corresponding measures of HHb were also lower, but the difference was not statistically significant (Table 1). There were no differences in the latency of the hemodynamic peak between the patients and controls (mean time-to-peak O<sub>2</sub>Hb: 15.1 ± 4.7 s vs 11.6 ± 7.2 s; mean time-to-peak HHb: 13.2 ± 4.2 vs 11.4 ± 4.4 s). Figures 2a, d show the functional maps obtained by means of GLM, which indicate significant activations in the contralateral central area of both O<sub>2</sub>Hb and HHb signals.

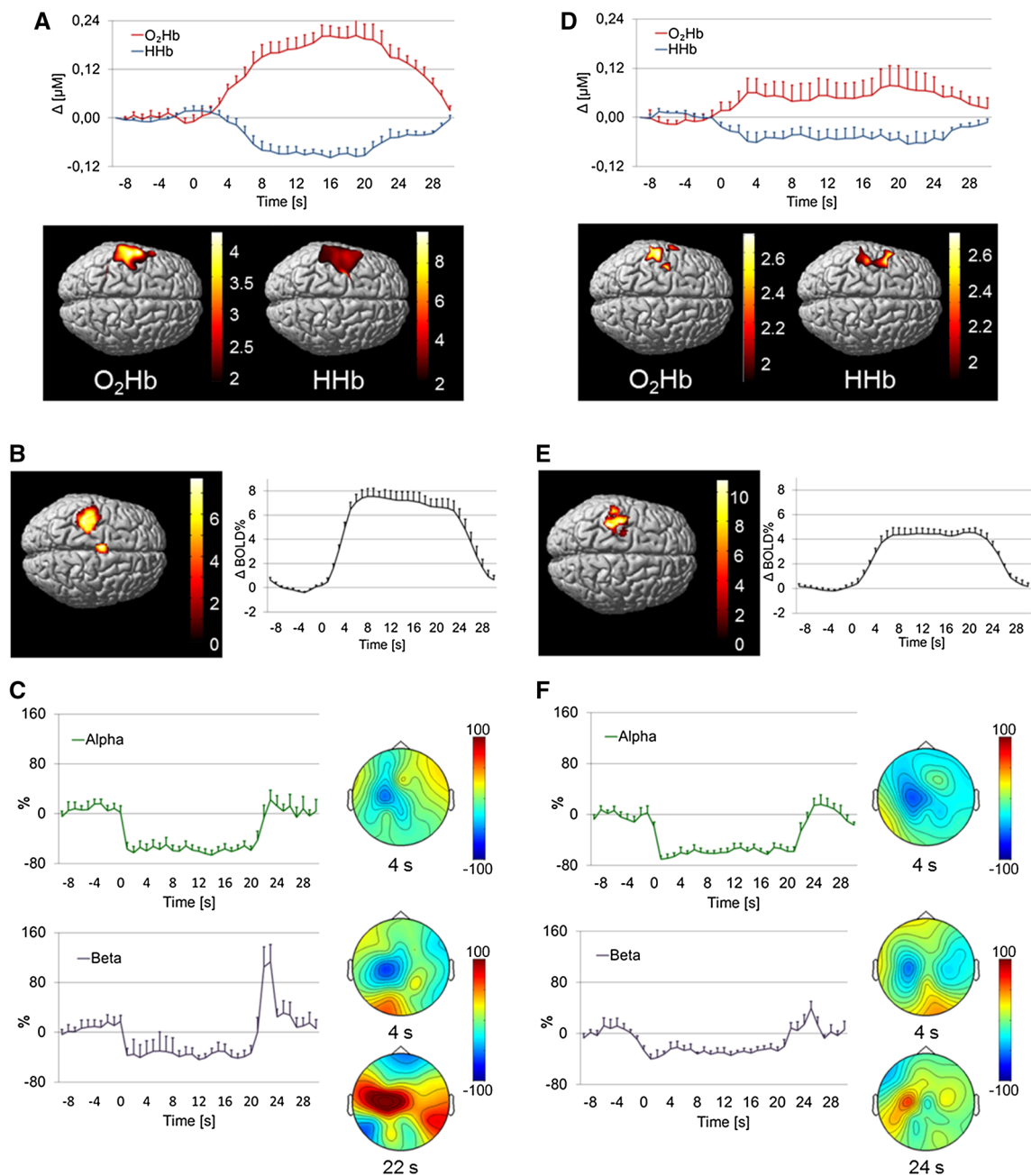


**Fig. 2** Group analyses of TD-fNIRS, fMRI and EEG data showing the effect of right handgrip for healthy subjects (*left box*) and EPM1-patients (*right box*). **a, d:** O<sub>2</sub>Hb and HHb time courses in the most reactive channel and the corresponding GLM activation maps

( $p < 0.05$ , uncorrected). **b, e:** fMRI activation maps ( $p < 0.05$ , uncorrected) and BOLD time course extracted from the active cluster. **c, f:** ERD/ERS time courses (C3 electrode) and maps in the alpha and beta bands. The *vertical bars* represent the standard error

## CT Analysis

Parcel-wise CT analysis revealed a significant reduction in the thickness of the pre-central and para-central areas bilaterally, and the right post-central area in the EPM1 patients (Table 1). Other thinned cortical regions were the left pars opercularis, the right inferior parietal area, and the

lateral occipital areas ( $p < 0.0004$ ). This was confirmed by vertex-wise CT analysis, which revealed six clusters surviving the Monte Carlo correction for multiple comparisons, with reduced CT in the EPM1 patients: the most significant clusters involved the pre-central gyrus bilaterally. Other clusters revealed thinning in the right superior temporal sulcus and in the right occipital lobe (left:

superior frontal and temporal, fusiform and rostral middle frontal areas; right: inferior parietal, transverse temporal, lateral occipital and superior frontal areas).

#### fMRI Data Analysis

The motor task elicited significant activation of the contralateral primary motor and somatosensory cortical areas in all of the subjects; it also elicited activation of the supplementary motor area in five controls and three EPM1 patients. In comparison with the resting condition, the movement indicated intense focal activity in the contralateral primary motor and somatosensory areas (peak significance at  $-36$ ,  $-21$  and  $54$  in the EPM1 patients, and  $-38$ ,  $-24$  and  $58$  in the controls). In addition, the averaged map of the controls also showed an activated cluster in the supplementary motor area (peak significance at  $-3$ ,  $-7$  and  $64$ ). The extension of the functional ROI was significantly smaller in the EPM1 patients ( $n^\circ$  voxels:  $1047.5 \pm 911.2$  vs  $2455.7 \pm 1579.1$ ,  $p = 0.030$ ).

Within the functional ROI, the time courses of the BOLD signals were similar to those obtained by means of TD-fNIRS: both signals showed an increase during the initial part of the task, a plateau during motor execution, and a return to the baseline 6–8 s. After the end of the movement ( $6.4 \pm 1$  s in the EPM1 patients, and  $6.8 \pm 1.5$  s in the controls). The maximal value and AUC of  $\Delta$ BOLD on the activated area were both significantly smaller in the EPM1 patients ( $5.17 \pm 1.21$  vs  $8.13 \pm 2.37$  (%·s),  $p = 0.004$ ; and  $741.57 \pm 209.24$  vs.  $1275.50 \pm 350.24$  (%·s),  $p = 0.001$ , Table 1; Fig. 2b, e). There was no difference in the latency of the hemodynamic peak between the patients and controls ( $6.6 \pm 1.7$  s vs  $6.4 \pm 1.1$  s).

#### ERD/ERS Analysis

EEG event-related desynchronization/synchronization analysis was performed on EEG signals acquired with both TD-fNIRS and fMRI. The comparison using Wilcoxon signed-rank test of each ERS/ERD parameter did not show any significant difference between the two conditions, therefore, for further analyses, we used the results obtained with EEG-TD-fNIRS acquisition.

In all subjects, maximal values of  $\alpha$ - and  $\beta$ -ERD/ERS were observed on the EEG traces recorded from electrode C3.

The EPM1 patients had  $\alpha$ -ERD patterns that were not statistically different from those of the controls, but their  $\beta$ -ERD pattern was significantly greater ( $-53.97 \pm 6.05$  vs  $-43.11 \pm 12.36$  %,  $p = 0.033$ ). The expected post-movement synchronisation in the  $\beta$  band was observed in

all of the controls, but was undetectable in one EPM1 patient and significantly smaller than in the controls in the remaining patients ( $66.36 \pm 23.24$  vs  $151.29 \pm 94.12$  %,  $p = 0.040$ , Fig. 2c, f). Accordingly, the AUC was significantly smaller in the EPM1 patients ( $124.77 \pm 52.8$  vs  $367.87 \pm 257.3$  ( $\mu$ V·s),  $p = 0.040$ ).

#### Correlations

Among the optically derived hemoglobin parameters, significant correlations were found between  $O_2$ Hb and HHb maximal values ( $\rho = -0.635$ ,  $p = 0.003$ ), and between  $O_2$ Hb and HHb AUC ( $\rho = 0.621$ ,  $p = 0.005$ ).  $O_2$ Hb AUC also correlated with  $\Delta$ BOLD % AUC ( $\rho = 0.550$ ,  $p = 0.015$ ) and the extension of the fMRI ROI ( $\rho = 0.651$ ,  $p = 0.005$ ), and there was a significant correlation between  $O_2$ Hb AUC and EEG  $\beta$ -ERD ( $\rho = -0.573$ ,  $p = 0.013$ ). Left para-central and pre-central CT values significantly correlated with both  $O_2$ Hb ( $\rho = 0.701$ ,  $p = 0.001$  and  $\rho = 0.573$ ,  $p = 0.013$ ) and BOLD AUC ( $\rho = 0.648$ ,  $p = 0.004$  and  $\rho = 0.705$ ,  $p = 0.001$ ).

#### Discussion

We used TD-fNIRS and fMRI to evaluate patients with cortical myoclonus and controls in order to investigate the hemodynamic dysfunctions coupled with the abnormal neuronal activities occurring in discrete neuronal pools in EPM1 patients, who typically present with neocortical hyperexcitability involving the sensorimotor areas (Canafoglia et al. 2004; Danner et al. 2009; Manganotti et al. 2001; Shibasaki and Hallet 2005), but mainly the motor cortex, the ultimate generator of the myoclonic jerks consistently elicited by active movement. The regular appearance of small segmental jerks with active movements allows reliable test conditions and precise measures in these patients. Various neurophysiological findings have shown that cortical myoclonus is related to excess EEG oscillations closely coupled with EMG bursts corresponding to the jerks (Panzica et al. 2003). The mechanisms responsible for neuronal synchronisation are still unclear, but evidence obtained by means of transcranial magnetic stimulation protocols indicate a prominent impairment of intracortical inhibition (Manganotti et al. 2001; Canafoglia et al. 2010), a defect that is in line with data obtained in the mouse model of the disease that suggest decreased GABA-mediated inhibition (Buzzi et al. 2012).

In previous studies of EPM1 patients, we have found a clear and consistent change of the EEG rhythms in response to individual active movement (Visani et al. 2006) mainly leading to a reduction in post-movement  $\beta$



synchronisation that typically marks the end of a motor task in healthy subjects (Pfurtscheller and Lopes da Silva 1999). The same finding was obtained using “blocks” of movements (Visani et al. 2011), whereas concomitant fMRI did not reveal any significant differences in the activation maps or BOLD time course extracted from fixed structural ROIs. In this study, we used a different approach for detecting the hemodynamic changes occurring during a motor task that is based on evaluating hemodynamic and EEG parameters over the most activated region on the contralateral primary motor and somatosensory areas, which we considered a “functional ROI” as it was consistently activated by movement in all of the subjects. Therefore, we focused on the functionally activated area maximizing the useful information and not on preselected structural areas. In this way, we not only found the typical EEG pattern distinguishing EPM1 patients from controls (almost absent  $\beta$  ERS), but also significant differences in the BOLD and TD-fNIRS curves, both of which were significantly reduced in EPM1 patients.

#### Relationships Between BOLD and TD-fNIRS Signals

The hemodynamic profiles revealed by fMRI and TD-fNIRS were consistent in the EPM1 patients and controls, thus indicating that both methods are similarly capable of identifying the neurovascular changes occurring during a motor task under physiological and pathological conditions. The position of the TD-fNIRS optodes prevented us from exploring the activation of the supplementary motor area, but the GLM maps obtained using the fMRI and TD-fNIRS data showed an equivalent topography of the maximal hemodynamic change on the motor cortex (M1) contralateral to the activated hand, with little or no response in the surroundings regions.

The fNIRS and BOLD signals in both groups followed the course of the active movement, starting a few seconds after its beginning, lasting throughout its duration, and slowly decaying after its end (see Leff et al. 2011 for a review). The BOLD signal significantly correlated with the changes in  $O_2Hb$ , but not with the changes in  $HHb$ . A similar discrepancy has been previously observed in healthy subjects during motor (Anwar et al. 2013; Strangman et al. 2002) and cognitive tasks (Cui et al. 2011), and has been attributed to the higher signal-to-noise ratio of  $O_2Hb$  (Strangman et al. 2002). We also found that the  $HHb$  SNR was lower than that of  $O_2Hb$  in both the patients and controls, although an additional explanation could be the different origin of the hemoglobin signals, which are direct measure in the case of TD-fNIRS but indirectly derived from the decreased paramagnetic  $HHb$  content in the case of BOLD (Steinbrink et al. 2006).

#### Movement-Related EEG Changes and Hemodynamics

The block design of the task is unusual for ERD/ERS, which are classically studied using single event protocols; however, block tasks have been previously used successfully (Erbil and Urgan 2007; Visani et al. 2011) and the data were also consistent in this study. Using this type of stimulus, we obtained a reliable ERD/ERS pattern consisting of the modulation of oscillatory activity in the  $\alpha$  and  $\beta$  bands. The EPM1 patients and controls both showed a characteristic spatio-temporal profile of EEG  $\beta$  and  $\alpha$  ERD during movement preparation and execution, which is considered to reflect the activation of the specific cortical area involved in the task (motor in our case) (Pfurtscheller and Lopes da Silva 1999). The  $\beta$ -ERS that leads to a sharp rebound in  $\beta$  activity at the end of a movement was detectable in the controls but not in the patients. The mechanism and circuitries leading to  $\beta$ -ERS are still unclear, but it is thought to be due to inhibitory phenomena (Chen et al. 1998) and to reveal the return of the responsible neuronal populations to the inactive state.

The fact that the ERD/ERS changes explicitly revealing complex and uneven neuronal behaviour in the controls concurred with a monotonic hemodynamic response of both BOLD and TD-fNIRS suggests that the neuronal activities necessary for motor activation and conclusion give rise to a cumulative energy requirement, and that the hemodynamic signals were insensitive to the variable neuronal circuitries refining the movement. The hemodynamic signals in the EPM1 patients, who typically lack  $\beta$ -ERS, had a similar time course but were significantly lessened, possibly because of their mild cortical atrophy. Heinzel et al. 2013 have recently reported that up to 41 % of the variance in the  $HHb$  signal and up to 18 % of the variance in the  $O_2Hb$  signal in frontal regions can be explained by individual grey matter volume; moreover, differences in the distance between the scalp and cortex may affect the sensitivity of fNIRS (Haeussinger et al. 2011). As in previous studies of EPM1 patients (Koskenkorva et al. 2009, 2012), we found that motor area CT was moderately reduced in our patients, and correlated with the reduction in the hemodynamic signals.

When studying EPM1 patients, it need to be remembered that voluntary hand activation may be intermingled with small myoclonic jerks, thus leading to less fluid movement and possibly less cortical activation. However, it is unlikely that the reduced hemodynamic changes were due to the reorganisation of cortical circuitry which, even when it is associated with atrophic changes, leads to hyperexcitability phenomena and hypersynchronous oscillations (Panzica et al. 2003; Panzica et al. 2014). Energy requirement and oxygen consumption are highly dependent on the action potential rate (Attwell and Laughlin 2001),

and so it can be hypothesised that, in EPM1 patients, the loss of inhibitory neuronal components that typically fire at very high frequencies (e.g. interneurons) not only causes hyperexcitability, decreased intra-cortical inhibition (Shibasaki and Hallet 2005; Canafoglia et al. 2004; Canafoglia et al. 2010) and impaired  $\beta$ -ERS, but also reduces the metabolic requirement as reflected by the lower hemodynamic curves measured by means of TD-fNIRS and BOLD signals.

### Limitations

The study has some technical limitations. First of all, fMRI and TD-fNIRS were not simultaneously recorded although, in order to test the consistency of the hemodynamic data, the EEGs were recorded simultaneously with both. As the EEG analysis provided comparable results, it can be assumed that the functional mechanisms involved in the motor task were similar during the fMRI and TD-fNIRS measurements.

A second limitation of our approach may be the placement of the optodes. During EEG-TD-fNIRS recordings, some optodes were placed in the standard 10/20 standard positions and so the EEG electrodes were slightly delocalised; however, the relatively poor spatial resolution of EEG scalp recordings suggests that this is a minor issue. Moreover, the position of the TD-fNIRS optodes prevents investigation of the activation of the supplementary motor area. Future studies could explore different methods of recording EEGs and their extension to the supplementary motor cortex.

### Conclusion

We used fMRI to evaluate  $\Delta$ BOLD, TD-fNIRS to investigate changes in  $O_2$ Hb and HHb, and EEG ERD/ERS in the  $\alpha$  and  $\beta$  bands of ten patients with cortical action myoclonus due to progressive myoclonic epilepsy (EPM1) and 12 healthy controls who all performed ten blocks of repetitive hand grasping alternated with rest.

The fMRI and TD-fNIRS signals were consistent, significantly correlated, and showed lessened hemodynamic changes in the EPM1 patients. This may be partially attributable to their mild cortical thickening. However, cortical hyperexcitability, which is known to generate myoclonic jerks and probably explains the lack of EEG  $\beta$ -ERS, did not reflect an increase in energy requirement. We hypothesise that the loss of inhibitory neuronal components that typically fire at very high frequencies may account for the reduced metabolic requirement.

**Acknowledgments** This study received funding from the European Community's Seventh Framework Programme (FP7/2007-2013) under Grant agreement HEALTH-F5-2008-201076 (nEUROPt). The authors are grateful to Elena Schiaffi and Alice Granvillano for their outstanding technical assistance during EEG-TD-fNIRS and EEG-fMRI data acquisition.

### References

- Allen PJ, Polizzi G, Krakow K, Fish DR, Lemieux L (1998) Identification of EEG events in the MR scanner: the problem of pulse artefact and a method for its subtraction. *NeuroImage* 8(3):229–239
- Allen PJ, Josephs O, Turner R (2000) A method for removing imaging artefact from continuous EEG recorded during functional MRI. *NeuroImage* 12(2):230–239
- Anwar AR, Muthalib M, Perrey S, Galka A, Granert O, Wolff S, Deuschl G, Raethjen J, Heute U, Muthuraman M (2013) Comparison of causality analysis on simultaneously measured fMRI and NIRS signals during motor tasks. *Conf Proc IEEE Eng Med Biol Soc* 2013:2628–2631
- Attwell D, Laughlin SB (2001) An energy budget for signaling in the grey matter of the brain. *J Cereb Blood Flow Metab* 21(10):1133–1145
- Buzzi A, Chikhladze M, Falcicchia C, Paradiso B, Lanza G, Soukupova M, Marti M, Morari M, Franceschetti S, Simonato M (2012) Loss of cortical GABA terminals in Unverricht–Lundborg disease. *Neurobiol Dis* 47(2):216–224
- Canafoglia L, Ciano C, Panzica F, Scaioli V, Zucca C, Agazzi P, Visani E, Avanzini G, Franceschetti S (2004) Sensorimotor cortex excitability in Unverricht–Lundborg disease and lafora body disease. *Neurology* 63:2309–2315
- Canafoglia L, Ciano C, Visani E, Anversa P, Panzica F, Viri M, Gennaro E, Zara F, Madia F, Franceschetti S (2010) Short and long interval cortical inhibition in patients with Unverricht–Lundborg and lafora body disease. *Epilepsy Res* 89:232–237
- Chen R, Tam A, Butefisch C, Corwell B, Ziemann U, Rothwell JC, Cohen LG (1998) Intracortical inhibition and facilitation in different representations of the human motor cortex. *J Neurophysiol* 80:2870–2881
- Contini D, Torricelli A, Pifferi A, Spinelli L, Cubeddu R (2007) Novel method for depth-resolved brain functional imaging by time-domain NIRS. *Proc SPIE* 6629:662908
- Contini D, Spinelli L, Caffini M, Cubeddu R, Torricelli A (2009) A multichannel time-domain brain oximeter for clinical studies. *Proceedings of SPIE-OSA biomedical optics*, P 7369 1D
- Cui X, Bray S, Bryant DM, Glover GH, Reiss AL (2011) A quantitative comparison of NIRS and fMRI across multiple cognitive tasks. *Neuroimage* 54(4):2808–2821
- Danner N, Julkunen P, Khyuppenen J, Hukkanen T, Kononen M, Saisanen L, Koskenkorva P, Vanninen R, Lehesjoki AE, Kalviainen R, Mervaala E (2009) Altered cortical inhibition in Unverricht–Lundborg type progressive myoclonus epilepsy (EPM 1). *Epilepsy Res* 85(1):81–88
- Desikan RS, Segonne F, Fischl B, Quinn BT, Dickerson BC, Blacker D, Buckner RL, Dale AM, Maguire RP, Hyman BT, Albert MS, Killiany RJ (2006) An automated labeling system for subdividing the human cerebral cortex on MRI scans into gyral based regions of interest. *NeuroImage* 31:968–980
- Erbil N, Ungan P (2007) Changes in the alpha and beta amplitudes of the central EEG during the onset, continuation, and offset of long-duration repetitive hand movements. *Brain Res* 12(1169):44–56

- Fischl B, van der Kouwe A, Destrieux C, Halgren E, Segonne F, Salat DH, Busa E, Seidman LJ, Goldstein J, Kennedy D, Caviness V, Makris N, Rosen B, Dale AM (2004) Automatically parcellating the human cerebral cortex. *Cereb Cortex* 14:11–22
- Friston KJ, Holmes AP, Worsley KJ, Poline JB, Frith C, Frackowiak RSJ (1995) Statistical parametric maps in functional imaging: a general linear approach. *Hum Brain Mapp* 2:189–210
- Gray MA, Minati L, Harrison NA, Gianaros PJ, Napadow V, Critchley HD (2009) Physiological recordings: basic concepts and implementation during functional magnetic resonance imaging. *Neuroimage* 47(3):1105–1115
- Haeussinger FB, Heinzel S, Hahn T, Schecklmann M, Ehlis AC, Fallgatter AJ (2011) Simulation of near-infrared light absorption considering individual head and prefrontal cortex anatomy: implications for optical neuroimaging. *PLoS ONE* 6(10):e26377
- Han X, Jovicich J, Salat D, van der Kouwe A, Quinn B, Czanner S, Busa E, Pacheco J, Albert M, Killiany R, Maguire P, Rosas D, Makris N, Dale A, Dickerson B, Fischl B (2006) Reliability of MRI-derived measurements of human cerebral cortical thickness: the effects of field strength, scanner upgrade and manufacturer. *Neuroimage* 32:180–194
- Heinzel S, Haeussinger FB, Hahn T, Ehlis AC, Plichta MM, Fallgatter AJ (2013) Variability of (functional) hemodynamics as measured with simultaneous fNIRS and fMRI during intertemporal choice. *NeuroImage* 71:125–134
- Jang KE, Tak S, Jung J, Jang J, Jeong Y, Ye JC (2009) Wavelet minimum description length detrending for near-infrared spectroscopy. *J Biomed Opt* 14:034004
- Koskenkorva P, Khyuppenen J, Niskanen E, Könönen M, Bendel P, Mervaala E, Lehesjoki AE, Kälviäinen R, Vanninen R (2009) Motor cortex and thalamic atrophy in Unverricht–Lundborg disease: voxel-based morphometric study. *Neurology* 73(8):606–611
- Koskenkorva P, Niskanen E, Hyppönen J, Könönen M, Mervaala E, Soininen H, Kälviäinen R, Vanninen R (2012) Sensorimotor, visual, and auditory cortical atrophy in Unverricht–Lundborg disease mapped with cortical thickness analysis. *AJNR Am J Neuroradiol* 33(5):878–883
- Leff DR, Orihuela-Espina F, Elwell CE, Athanasiou T, Delpy DT, Darzi AW, Yang GZ (2011) Assessment of the cerebral cortex during motor task behaviours in adults: a systematic review of functional near infrared spectroscopy (fNIRS) studies. *Neuroimage* 54(4):2922–2936
- Logothetis NK, Pauls J, Augath M, Trinath T, Oeltermann A (2001) Neurophysiological investigation of the basis of the fMRI signal. *Nature* 412(6843):150–157
- Magaudda A, Gelisse P, Genton P (2004) Antimyoclonic effect of levetiracetam in 13 patients with Unverricht–Lundborg disease: clinical observation. *Epilepsia* 45(6):678–681
- Manganotti P, Tamburin S, Zanette G, Fiaschi A (2001) Hyperexcitable cortical responses in progressive myoclonic epilepsies: a TMS study. *Neurology* 57:1793–1799
- Panzica F, Canafoglia L, Franceschetti S, Binelli S, Ciano C, Visani E, Avanzini G (2003) Movement-activated myoclonus in genetically defined progressive myoclonic epilepsies: EEG–EMG relationship estimated using autoregressive models. *Clin Neurophysiol* 114(6):1041–1052
- Panzica F, Canafoglia L, Franceschetti S (2014) EEG–EMG information flow in movement-activated myoclonus in patients with Unverricht–Lundborg disease. *Clin Neurophysiol* 125(9):1803–1808
- Perrin F, Pernier J, Bertrand O, Echallier JF (1989) Spherical splines for scalp potential and current density mapping. *Electroencephalogr Clin Neurophysiol* 72:184–187
- Pfurtscheller G, Lopes da Silva FH (1999) EEG/EMG synchronization and desynchronization: basic principles. *Clin Neurophysiol* 110:1842–1857
- Segonne F, Pacheco J, Fischl B (2007) Geometrically accurate topology-correction of cortical surfaces using nonseparating loops. *IEEE Trans Med Imaging* 26:518–529
- Shahwan A, Farrell M, Delanty N (2005) Progressive myoclonic epilepsies: a review of genetic and therapeutic aspects. *Lancet Neurol* 4:239–248
- Shibasaka H, Hallet M (2005) Electrophysiological studies of myoclonus. *Muscle Nerve* 31:157–174
- Steinbrink J, Villringer A, Kempf F, Haux D, Boden S, Obrig H (2006) Illuminating the BOLD signal: combined fMRI–fNIRS studies. *Magn Reson Imaging* 24(4):495–505
- Strangman G, Culver JP, Thompson JH, Boas DA (2002) A quantitative comparison of simultaneous BOLD fMRI and NIRS recordings during functional brain activation. *NeuroImage* 17:719–731
- Torricelli A, Contini D, Pifferi A, Caffini M, Re R, Zucchelli L, Spinelli L (2014) Time domain functional NIRS imaging for human brain mapping. *NeuroImage* 85:28–50
- Virtaneva K, D’Amato E, Miao J, Koskiniemi M, Norio R, Avanzini G, Franceschetti S, Michelucci R, Tassinari CA, Omer S, Pennacchio LA, Myers RM, Dieguez-Lucena JL, Krahe R, de la Chappelle A, Lehesjoki AE (1997) Unstable minisatellite expansion causing recessively inherited myoclonus epilepsy, EPM1. *Nat Genet* 15(4):393–396
- Visani E, Agazzi P, Canafoglia L, Panzica F, Ciano C, Scaiola V, Avanzini G, Franceschetti S (2006) Movement-related desynchronization–synchronization (ERD/ERS) in patients with Unverricht–Lundborg disease. *Neuroimage* 33(1):161–168
- Visani E, Minati L, Canafoglia L, Gilioli I, Granvillano A, Varotto G, Aquino D, Fazio P, Bruzzone MG, Franceschetti S, Panzica F (2011) Abnormal ERD/ERS but unaffected BOLD response in patients with Unverricht–Lundborg disease during index extension: a simultaneous EEG–fMRI study. *Brain Topogr* 24(1):65–77
- Ye JC, Tak S, Jang KE, Jung J, Jang J (2009) NIRS–SPM: statistical parametric mapping for near-infrared spectroscopy. *Neuroimage* 44(2):428–447 Epub 2008 Sep 12